Electronic Supplementary Material (ESI) for Journal name.

Supporting Information

All-Solid-State Three-Electrode Cells Enabling Diagnosis for Failure Modes

Young Jin Nam,[a,b] Kern Ho Park,[a] Dae Yang Oh,[a,b] Woo Hyun An[a] and Yoon Seok Jung*[a]

[a] *Department of Energy Engineering, Hanyang University, Seoul 04763, South Korea*

[b] *School of Energy and Chemical Engineering, Department of Energy Engineering, Ulsan National Institute of Science and Technology (UNIST), 50 UNIST-gil, Ulsan 44919, Republic of Korea*

*E-mail: yoonsjung@hanyang.ac.kr

Supporting Experimental

The Sn electrode for liquid-electrolyte-cells was prepared by spreading the Sn powders, super P, and poly(acrylic acid) (PAA) binder on a piece of Cu foil in a weight ratio of 70:10:20. The mass of Sn electrode was 4.7 $mg_{electrode}$ cm^{-2} (3.3 mg_{Sn} cm^{-2}). For the liquid-electrolyte-cell tests, 2032-type coin cells using Li metal as the counter and reference electrode were used. A solution of $LiPF_6$ (1.0 M) dissolved in a mixture of ethylene carbonate (EC), ethyl methyl carbonate (EMC), and dimethyl carbonate (DMC) (3:4:3 v/v) (Panax Etec) was used as the electrolyte. A porous polypropylene (PP)/polyethylene (PE)/PP tri-layer film (Celgard Inc.) was used as the separator. For the NCM/Li all-solid-state cells, the wet-slurry fabricated NCM electrodes, 120 μm Li metal foils (HONJO METAL), and the Li_6PS_5Cl pellet as the SE layer were used.

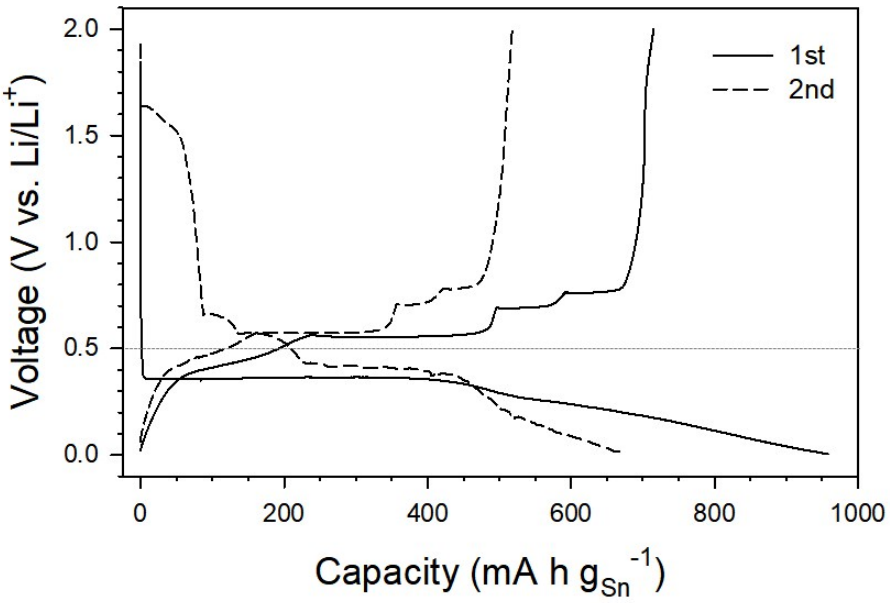

Fig. S1 First two-cycle discharge-charge voltage profiles Sn/Li cells using liquid electrolytes at 0.054 and 0.27 mA cm^{-2} at the first and second cycle, respectively.

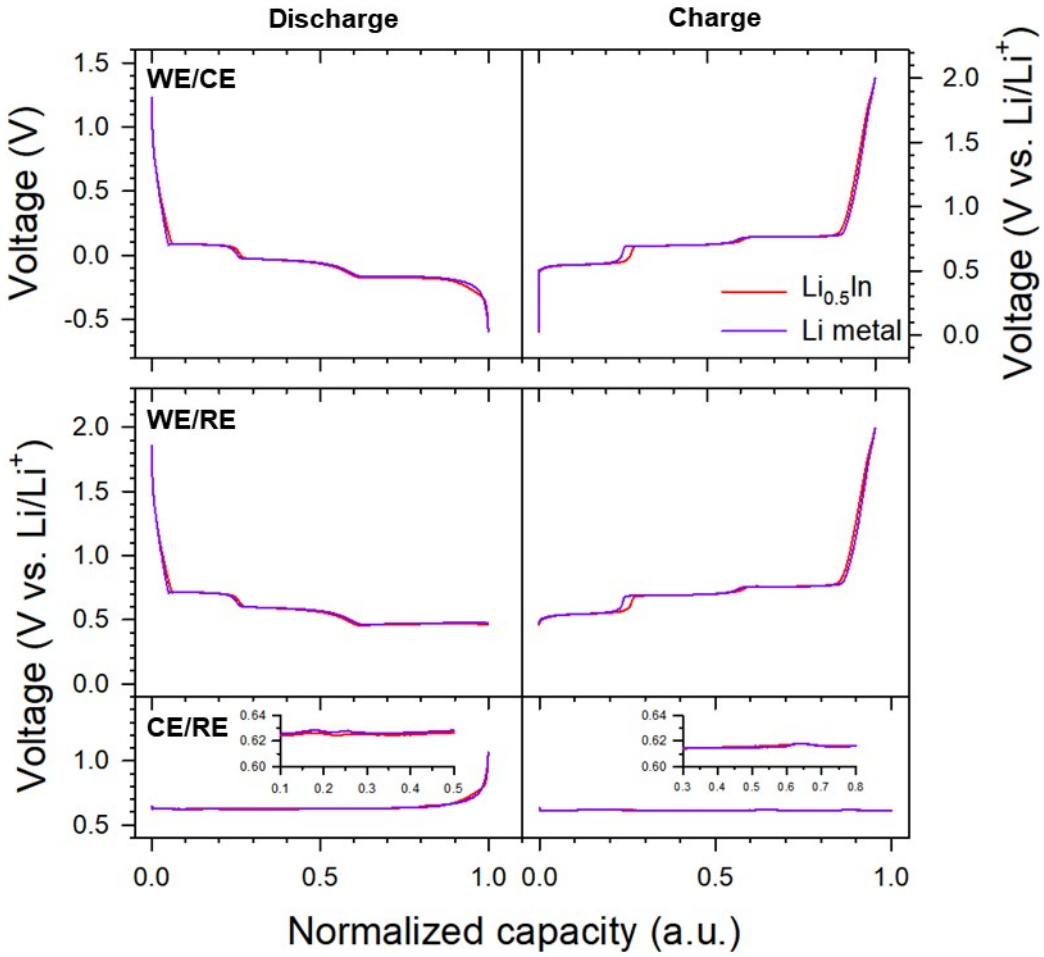

Fig. S2 Comparison of the discharge-charge voltage profiles of each electrode for Sn/Li-In all-solid-state three-electrode cells using $Li_{0.5}In$ or Li metal as REs.

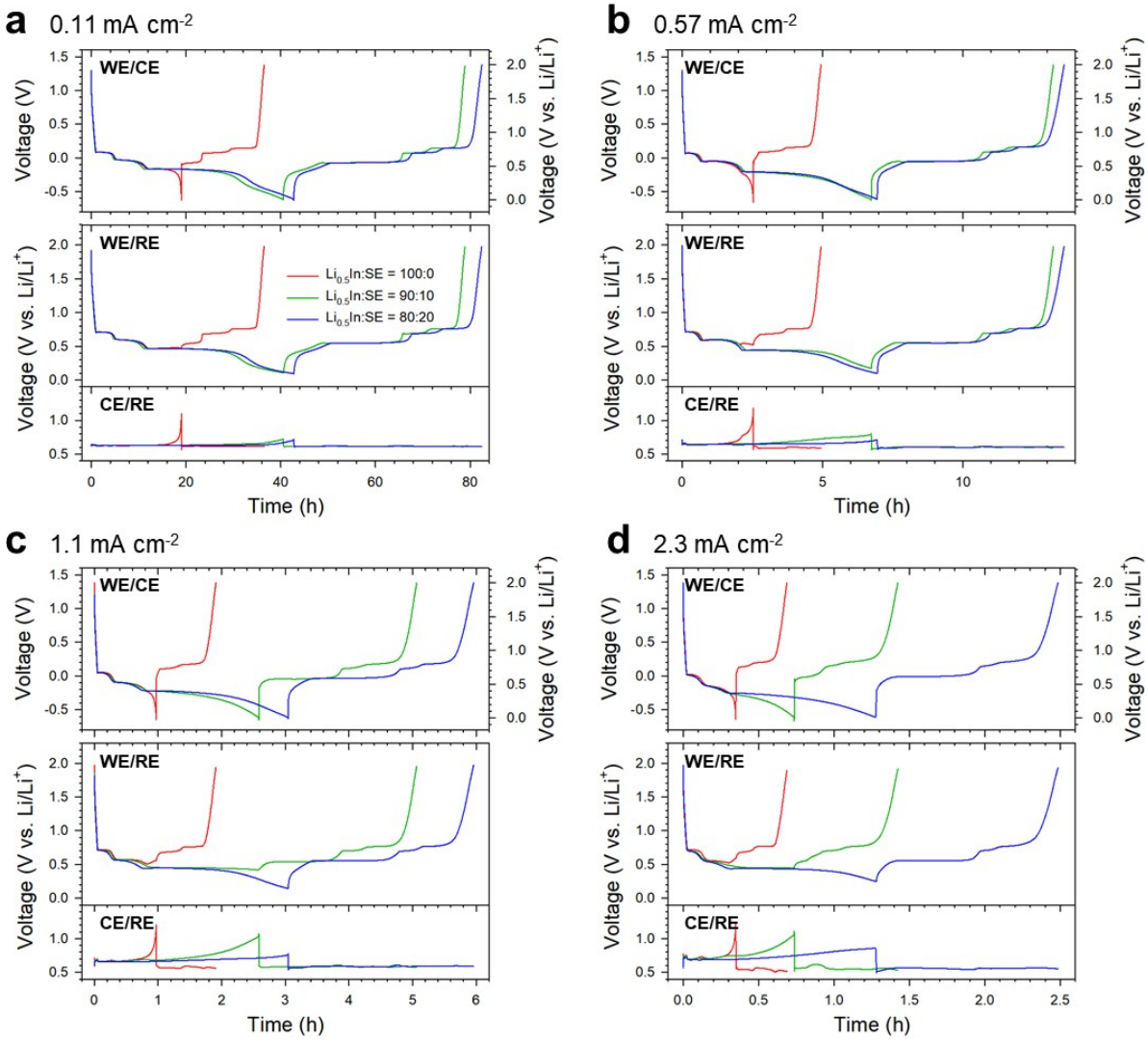

Fig. S3 Discharge-charge voltage profiles of each electrode for Sn/Li-In all-solid-state three-electrodes with different CEs using three different weight ratios of $Li_{0.5}In$/SE. The results of cycling at four different current densities are shown. Fig. 3b corresponds with (a).

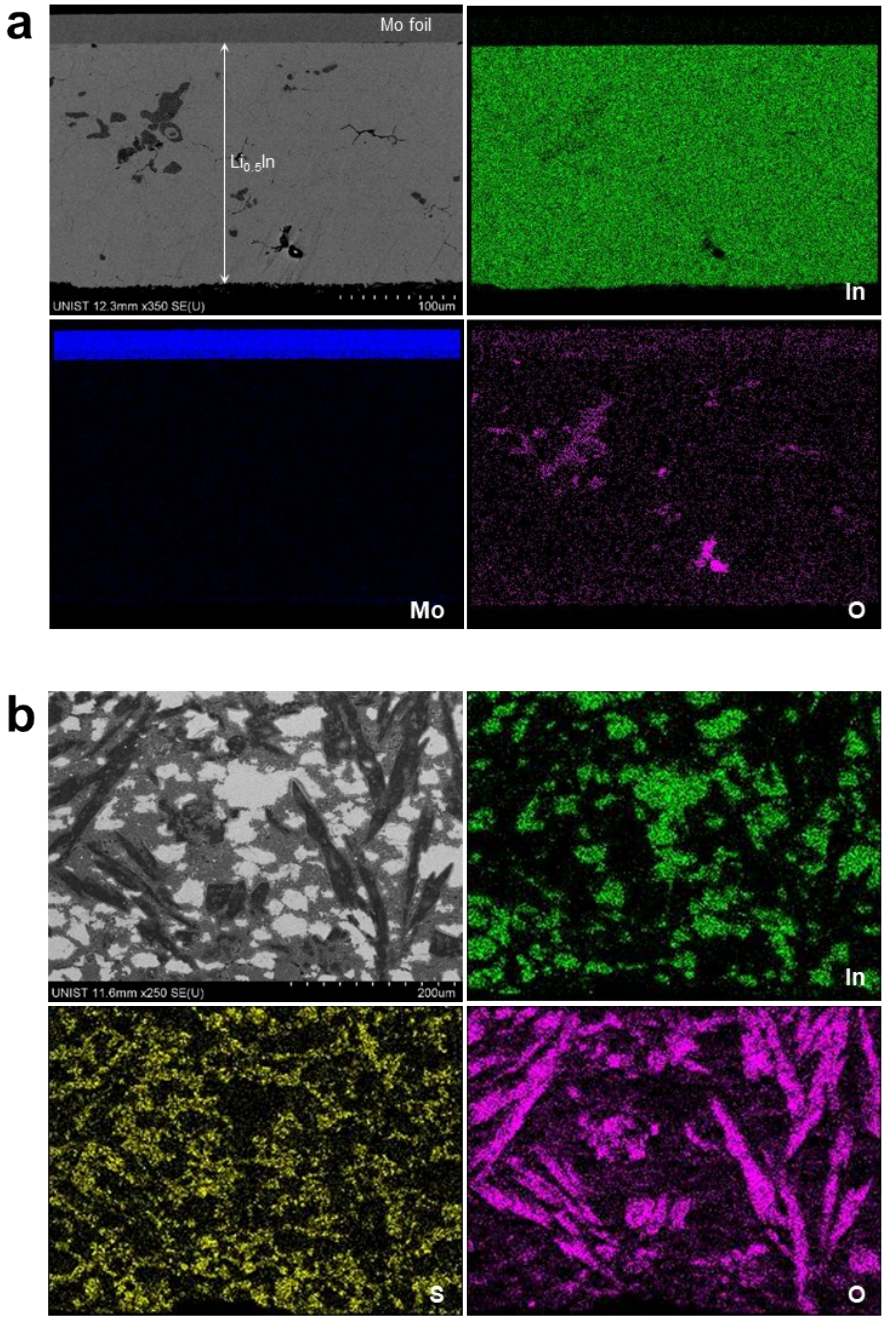

Fig. S4 Cross-sectional FESEM images for a) $Li_{0.5}In$ and b) $Li_{0.5}In$-SE (20 wt% of SE) CEs and their corresponding EDXS elemental maps.

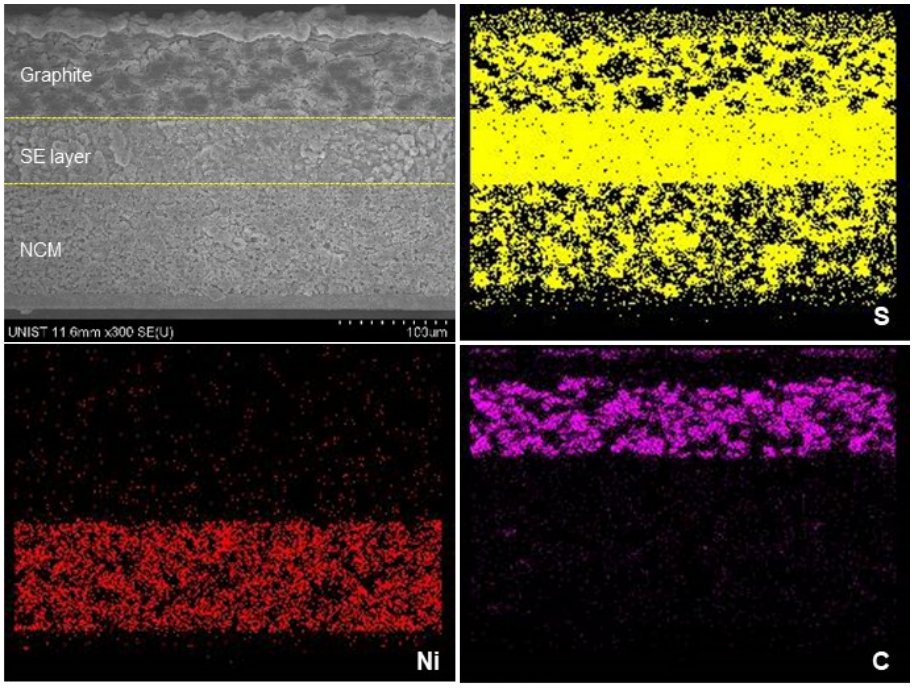

Fig. S5 Cross-sectional FESEM images and the corresponding EDXS elemental maps for NCM/Gr all-solid-state full-cells using thin SE layer (50–60 μm).

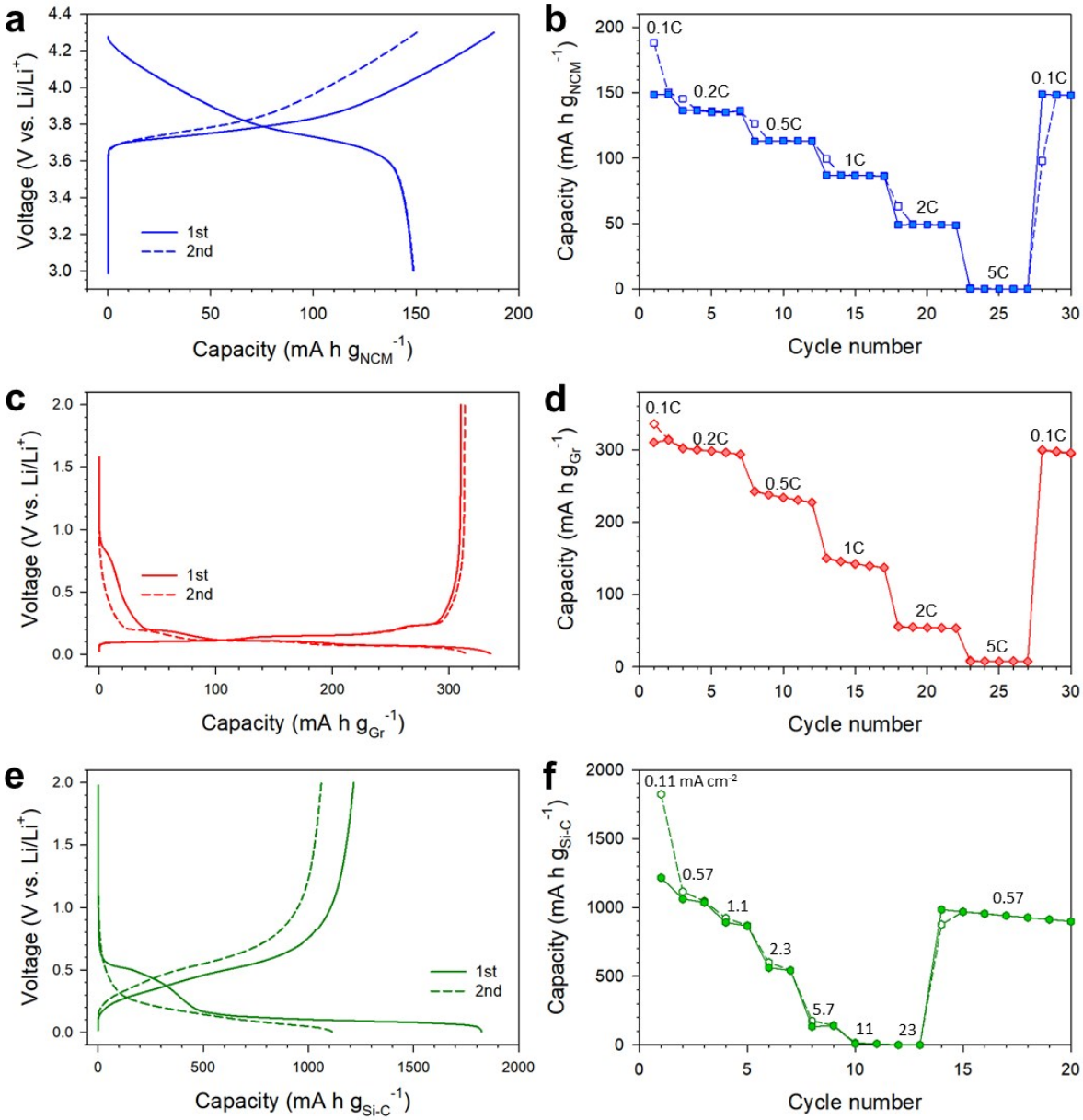

Fig. S6 Electrochemical performances of NCM/Li-In, Gr/Li-In-SE, and Si-C/Li-In-SE all-solid-state cells. First two-cycle voltage profiles of a) NCM/Li-In, c) Gr/Li-In-SE, and e) Si-C/Li-In-SE all-solid-state cells at 0.1C, 0.1C, and 0.11 mA cm^{-2}, respectively. The corresponding rate capabilities for a) NCM/Li-In, c) Gr/Li-In-SE, and e) Si-C/Li-In-SE all-solid-state cells are shown.

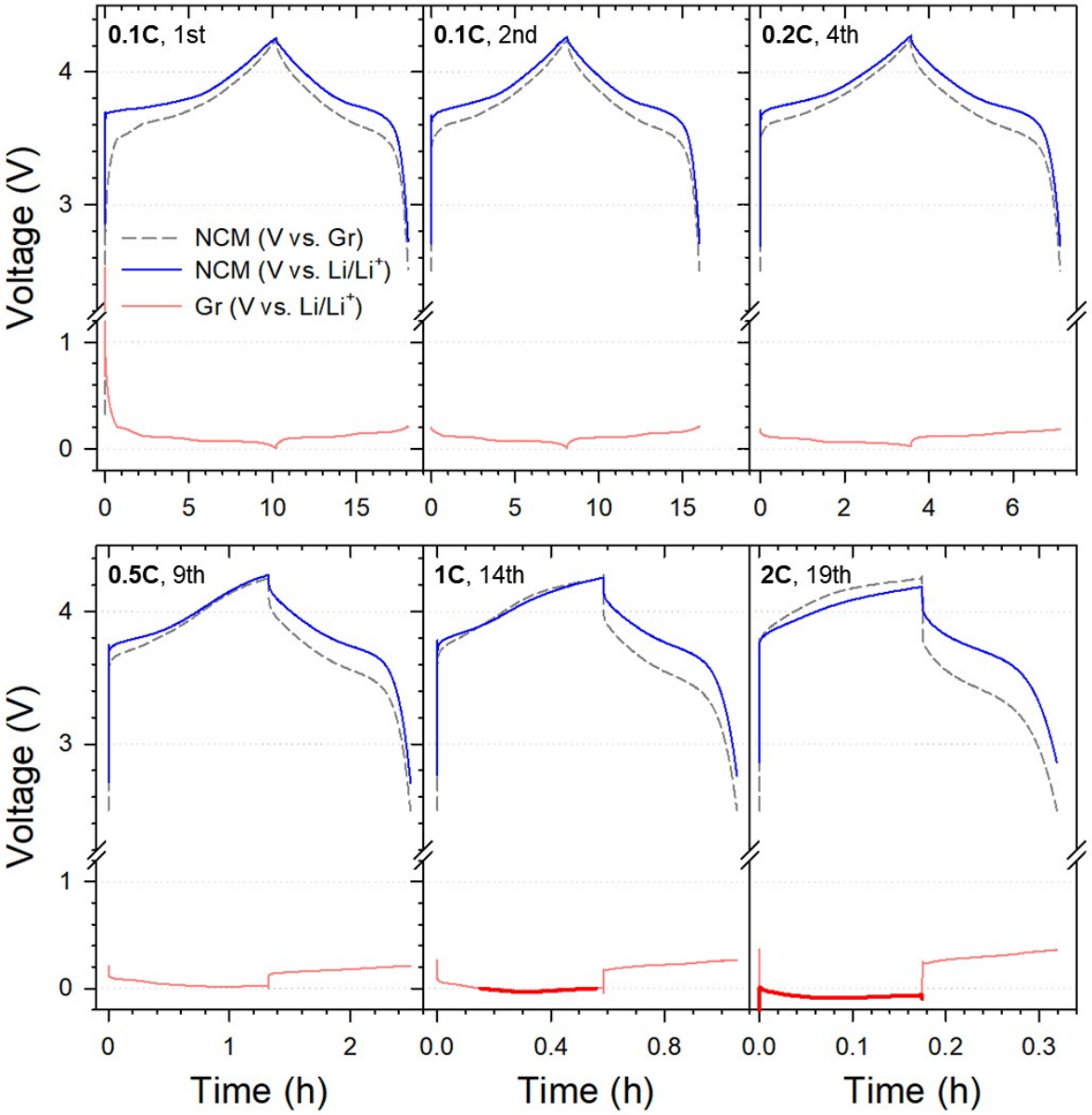

Fig. S7 Transient charge-discharge voltage profiles of each electrode for NCM/Gr all-solid-state three-electrode cells at different current densities. Note the voltage region of Gr, which is lower than 0 V (vs. Li/Li^+) at high C-rate, 1C, shown in bold red line.

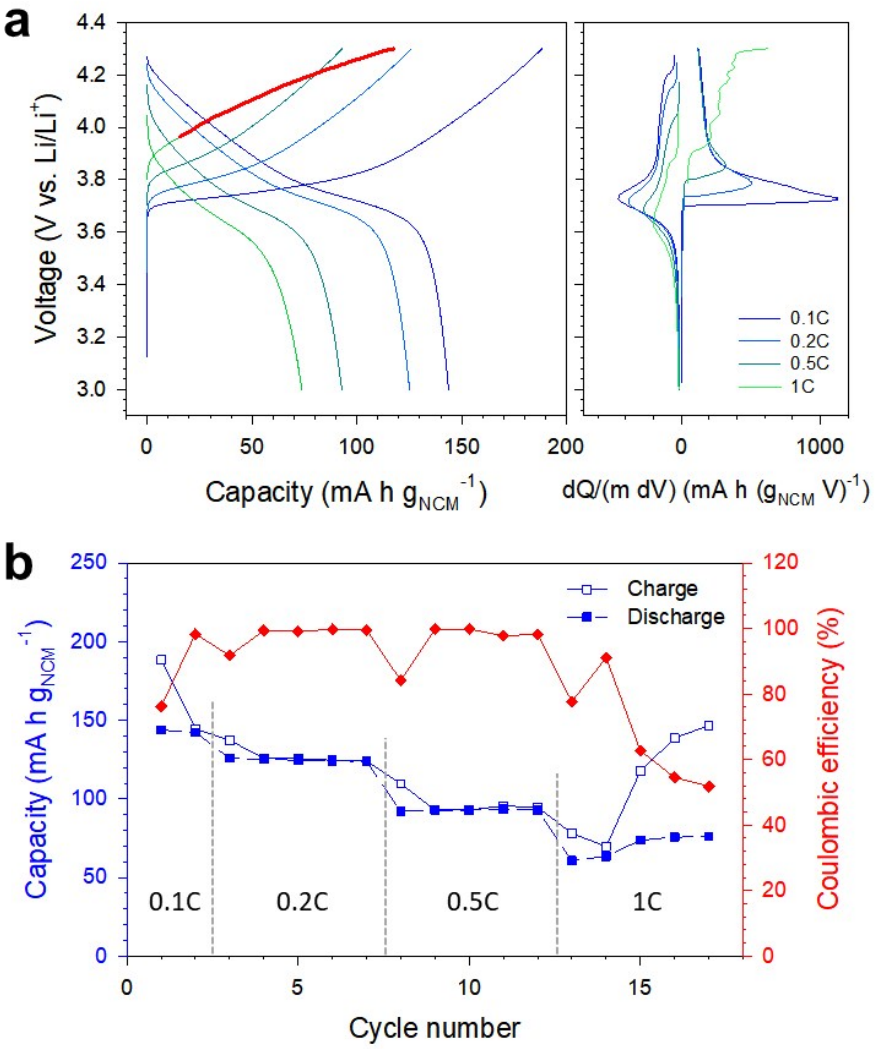

Fig. S8 a) Charge-discharge voltage profiles and their corresponding differential capacity plots for NCM/Li all-solid-state cells at 30 °C and various C-rates. b) Charge and discharge capacity varied by C-rates and the corresponding Coulombic efficiency as a function of cycle number. Note the abnormal plateau plotted in red at 1C in (a) and the corresponding low Coulombic efficiencies in (b), indicating the soft ISC by penetrating growth of Li metal.

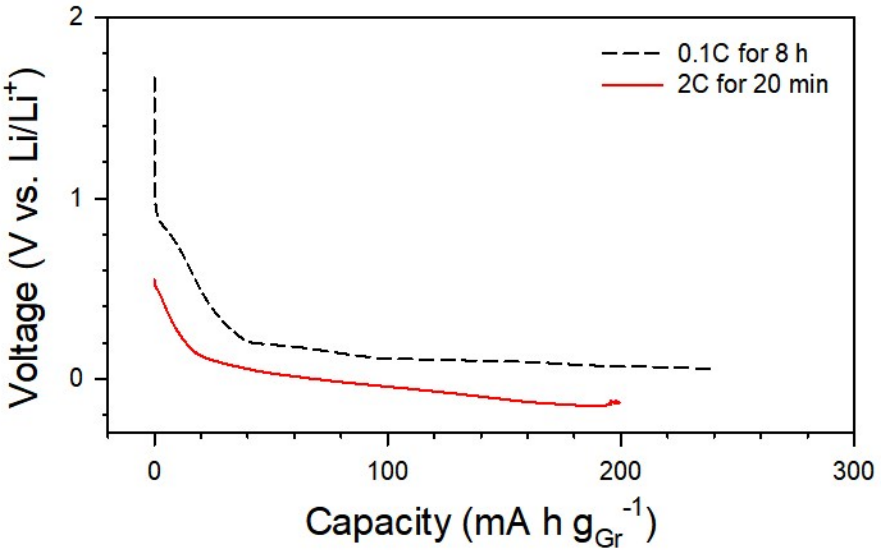

Fig. S9 First-cycle discharge (lithiation) voltage profiles for Gr/Li-In all-solid-state cells at different C-rates, which were used for ^{7}Li MAS NMR spectroscopy measurements (Fig. 5c). After the discharge, the mixtures of SE layers and Gr electrodes, collected from the disassembled cells, were subjected to the ^{7}Li MAS NMR spectroscopy measurements.

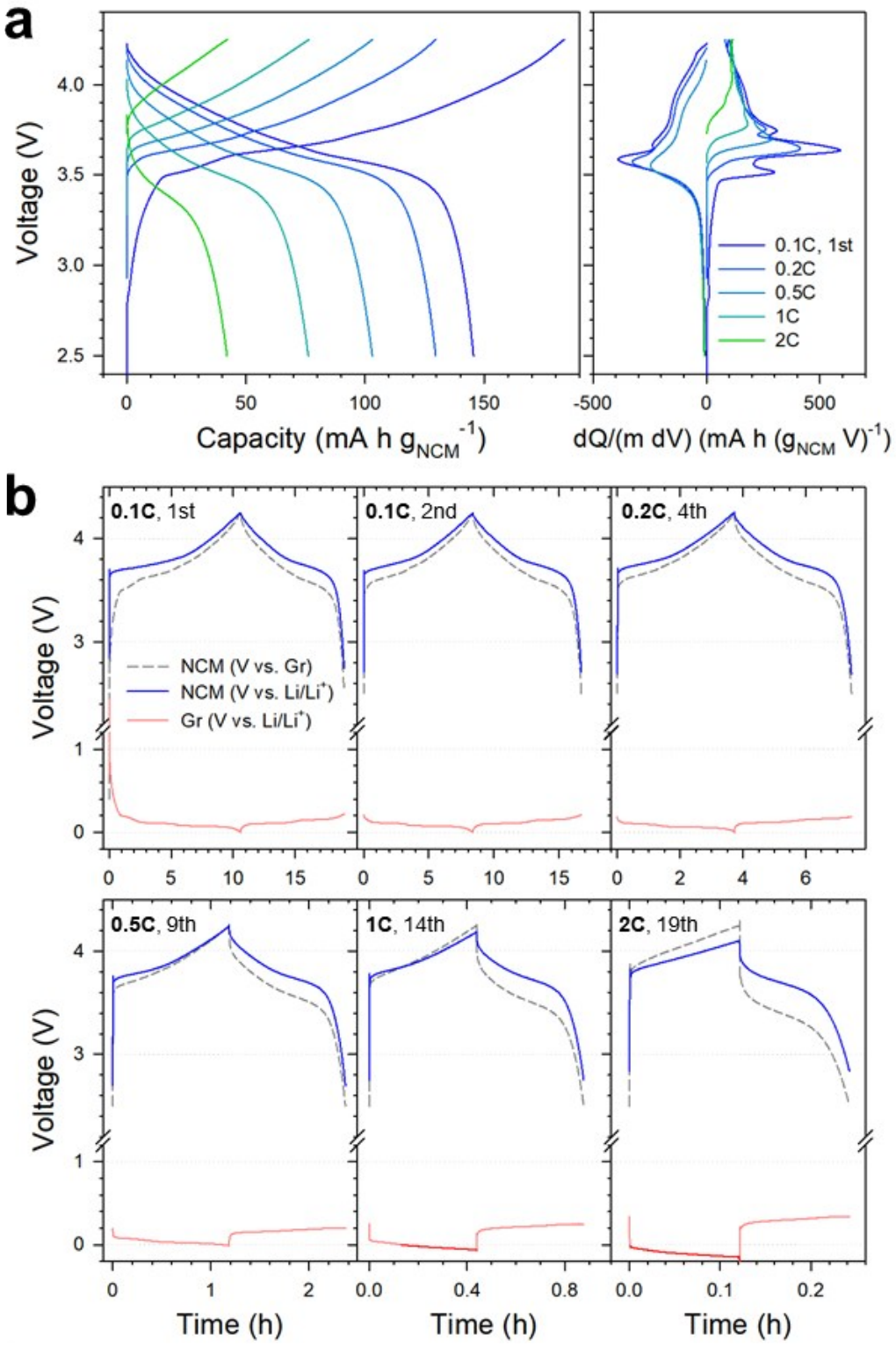

Fig. S10 Results for NCM/Gr all-solid-state three-electrode cells employing thick SE layers (730 μm), being free from ISC. a) Charge-discharge voltage profiles and the corresponding differential capacity plots at different C-rates. b) Charge-discharge voltage profiles for each electrode at different C-rates. Note the voltage region of Gr which is lower than 0 V (vs. Li/Li$^+$) at high C-rate, 1C, shown in bold red line.

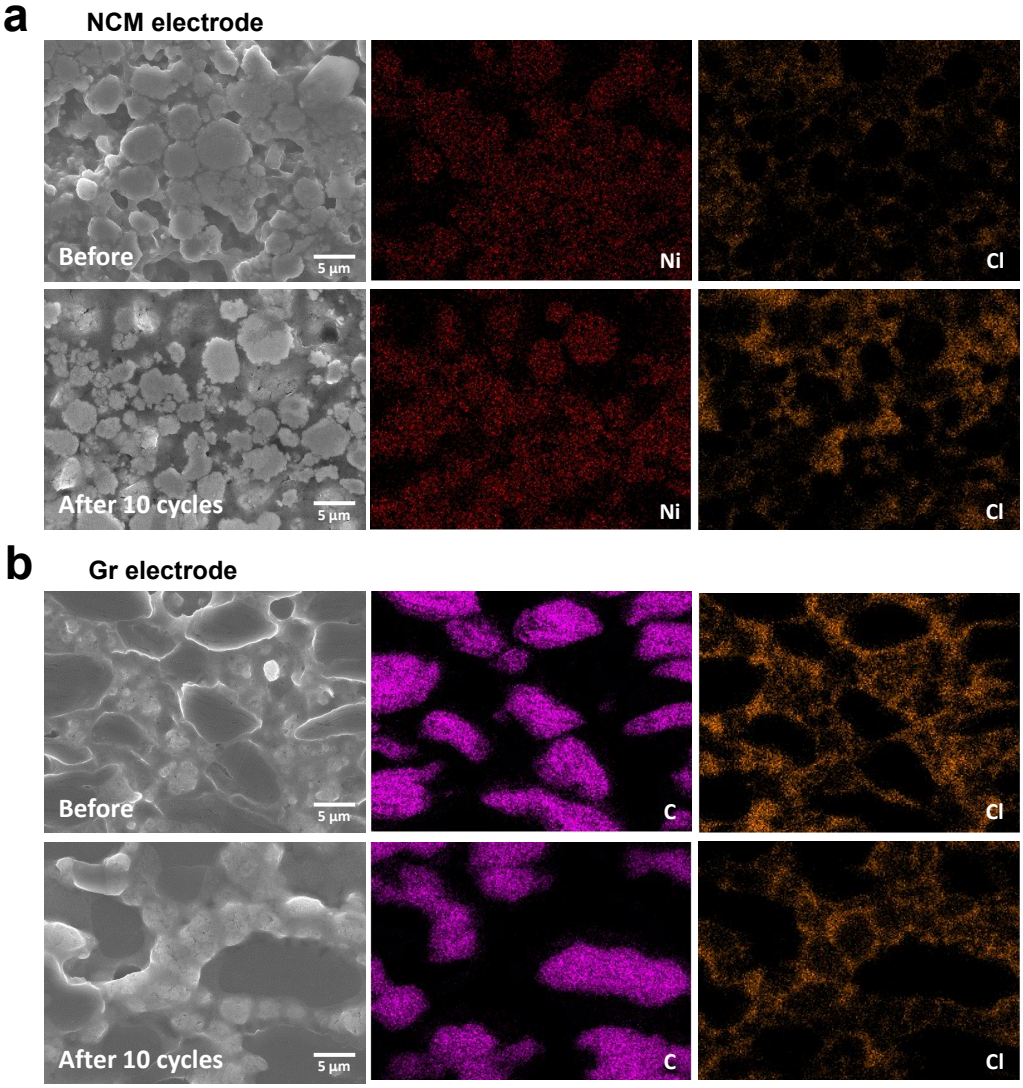

Fig. S11 Cross-sectional FESEM images and their corresponding EDXS elemental maps for a) NCM and b) Gr electrodes of NCM/Gr all-solid-state full-cells using thin SE layer (50–60 μm) before cycling and after 10 cycles at 0.2C.

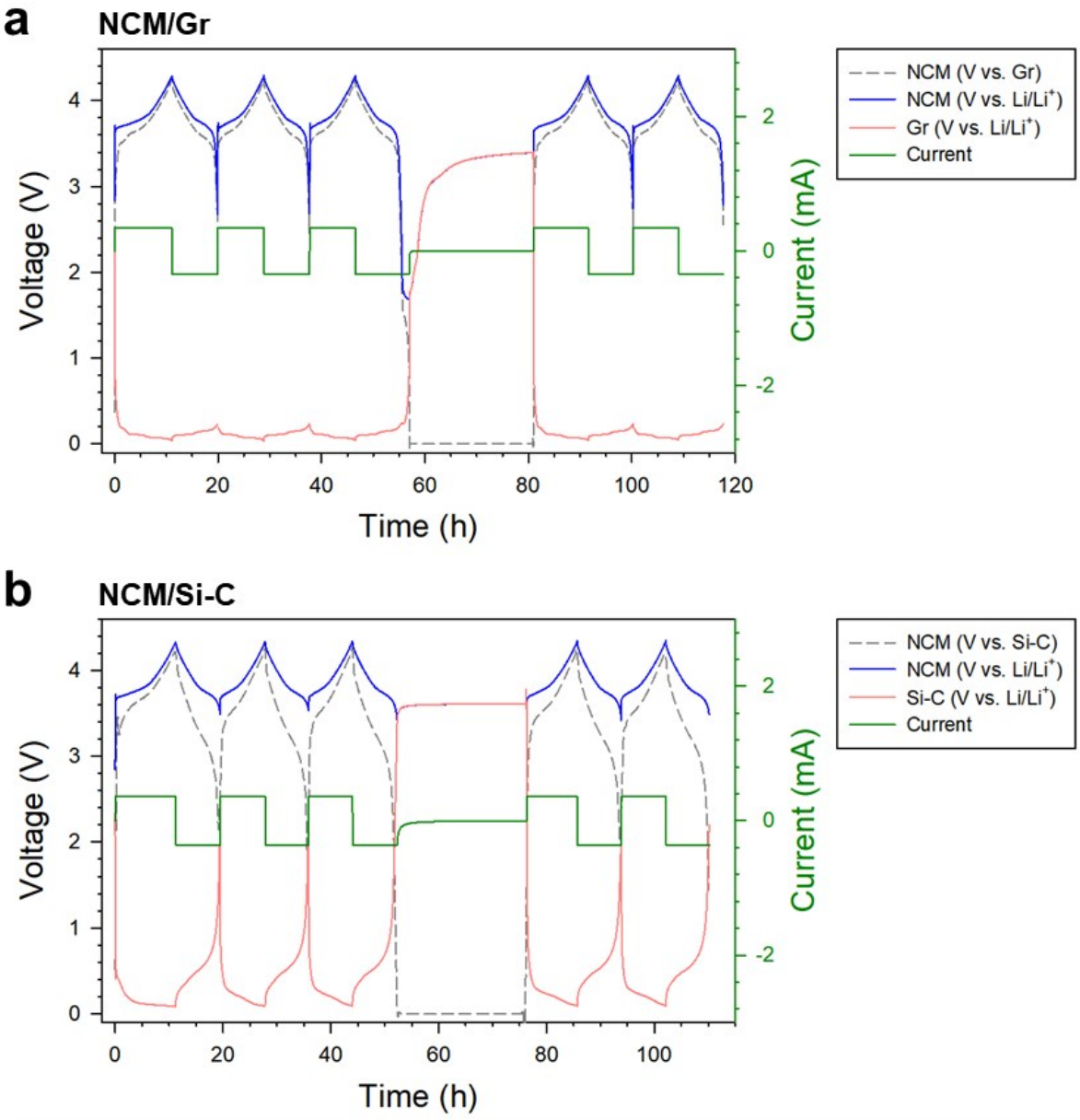

Fig. S12 Transient charge-discharge voltage profiles of each electrode for a) NCM/Gr and b) NCM/Si-C all-solid-state three-electrode cells during discharge to 0 V. Fig. 6 is the enlarged view in x-axis.

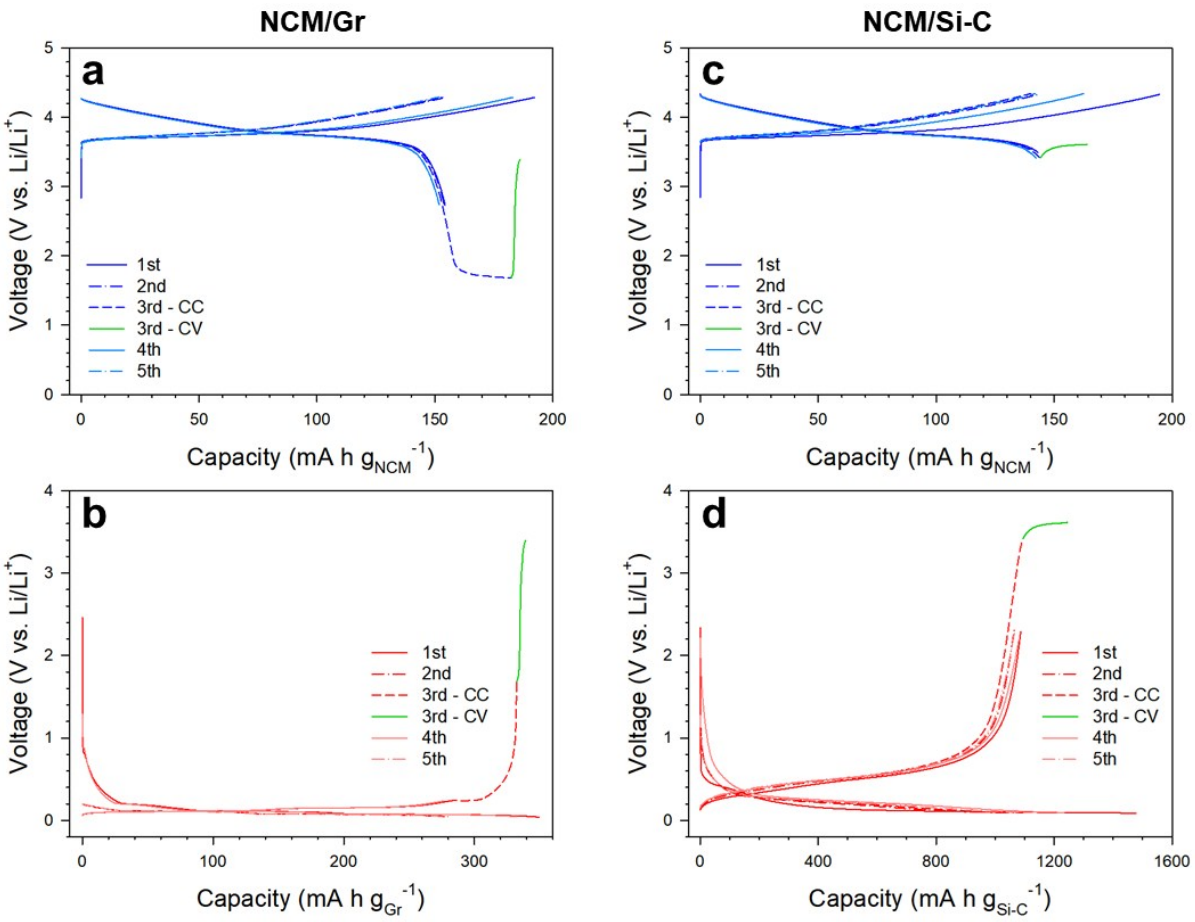

Fig. S13 Charge-discharge voltage profiles of a, c) NCM electrodes, b) Gr electrode, and d) Si-C electrode for NCM/Gr or NCM/Si-C all-solid-state three-electrode cells during discharge to 0 V.

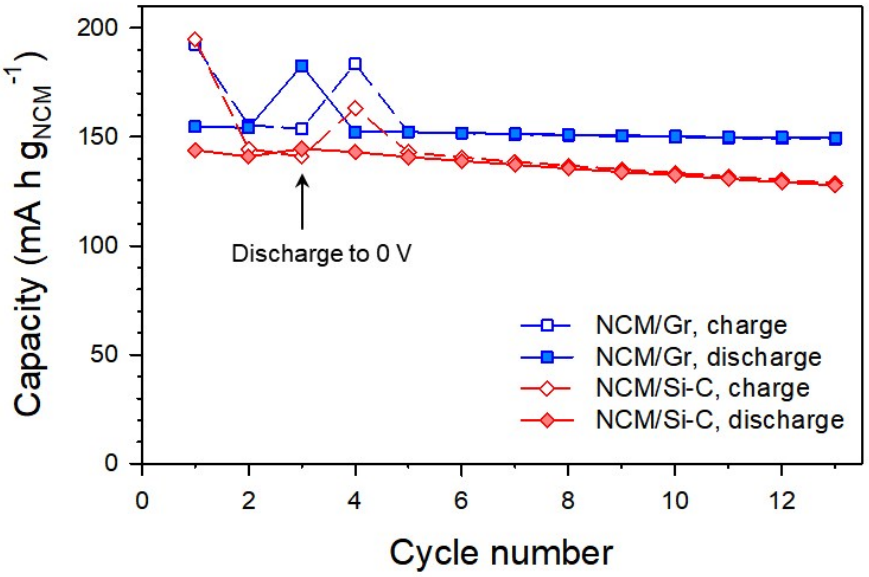

Fig. S14 Cycling performances of NCM/Gr and NCM/Si-C all-solid-state cells during discharge to 0 V. The corresponding charge-discharge voltage profiles are shown in Fig. 6, S12, S13.